

Development of Microtitre Plates for Electrokinetic Assays

J P H Burt^{1,2}, A D Goater², A Menachery¹, R Pethig¹, N H Rizvi²

¹School of Informatics, University of Wales, Bangor, Dean Street, Bangor, Gwynedd LL57 1UT, United Kingdom

²UK Laser Micromachining Centre, Dean Street, Bangor, Gwynedd, LL57 1UT, United Kingdom

burt@informatics.bangor.ac.uk

Abstract. Electrokinetic processes have wide ranging applications in microsystems technology. Their optimum performance at micro and nano dimensions allows their use both as characterization and diagnostic tools and as a means of general particle manipulation. Within analytical studies, measurement of the electrokinesis of biological cells has the sensitivity and selectivity to distinguish subtle differences between cell types and cells undergoing changes and is gaining acceptance as a diagnostic tool in high throughput screening for drug discovery applications. In this work the development and manufacture of an electrokinetic-based microtitre plate is described. The plate is intended to be compatible with automated sample loading and handling systems. Manufacturing of the microtitre plate, which employs indium titanium oxide microelectrodes, has been entirely undertaken using excimer and ultra-fast pulsed laser micromachining due to its flexibility in materials processing and accuracy in micro structuring. Laser micromachining has the ability to rapidly realize iterations in device prototype design while also having capability to be scaled up for large scale manufacture. The verification is achieved by the measurement of the electrorotation and dielectrophoretic properties of yeast cells while the flexibility of the developed microtitre plate is demonstrated by the selective separation of live yeast from polystyrene microbeads.

1. Introduction

Microtitre plates, or microtitration trays as they are sometimes called, are a standard tool in analytical biochemical research and clinical diagnostic testing laboratories. They essentially consist of a disposable, flat plastic plate, into which multiple 'wells' have been fabricated. These wells are used as small test tubes, and a plate typically has 6, 24, 96, 384, 1536 or even 6144 sample wells arranged in a 2:3 rectangular matrix. So, for example, 96 different reactions can be performed simultaneously on a single platform. The format is flexible and allows any combination of different or repeat reactions on any part of the plate. Reaction progress or end results monitoring is usually based on a color or fluorescence change allowing each well to be optically interrogated using automated plate reading equipment, which, when combined with robotic plate loading equipment allows experiments to be completely automated and capable of high throughput analysis. Increasingly, researchers are using non-colorimetric monitoring of reactions or are examining samples containing cells or cell populations. This has led to an evolution in the microtitre platform to include custom plates and make

use of different monitoring technologies, but employ the same automated sample handling and processing equipment.

An area of biotechnology that has seen significant growth in the past decade is that of AC electrokinetics [1] where AC electric fields are used to manipulate, characterize and analyze biological cells. The two most common electrokinetic techniques are dielectrophoresis and electrorotation. In dielectrophoresis non-uniform AC electric fields are used to selectively attract or repel cells from microelectrode arrays. In electrorotation a uniform, rotating, field is used to impart a rotational motion on cells. The direction and speed of electrokinesis is a function of the electrical permittivity and conductivity of the cell and its suspending medium along with the electric field geometry and strength. Simplistically, biological cells can be thought of as comprising of defined electrical regions such as the membrane, cytoplasm and nucleus. Since each region will have different electrical properties, interfacial polarization and relaxation processes cause the magnitude and direction of both dielectrophoretic and electrorotational motion to be electric field frequency dependent. Particle characterization and manipulation can be achieved by examining or exploiting the motion of cells under the influence of electric fields of one or more frequencies. An example of this is the separation of yeast cells from polystyrene microbeads. In low conductivity media ($<50\mu\text{S}/\text{cm}$) and low frequency electric fields ($<100\text{kHz}$), the high effective conductivity of the yeast cell wall makes it more polarizable than its suspending media and so experiences a positive force towards regions of high field strength, which generally occur at the edges of electrodes. In contrast, the low conductivity of the polymer microbeads causes them to be less polarizable than the suspending media and so they experience a negative force away from high field regions. The net effect is the physical separation of the two particle types into defined locations within an electrode system. While dielectrophoresis can be used for both particle characterization and manipulation, electrorotation is generally used as a characterization and diagnostic tool. Frequency dependent changes in the polarizability of the particle and medium cause particles to either rotate in a co-field or anti-field direction. Each particle type will exhibit characteristic peaks in its rotation spectrum along with crossover frequencies from co-field to anti-field rotation. By examining changes in the rotation spectrum of cells changes in their physico-chemical can be detected [2].

Laser micromachining [3], as a manufacturing technique, emerged from the development of micro and nanotechnologies over the past decade. While laser micromachining is still considered a new process in many areas of microengineering, it has become an established manufacturing method in niche applications areas such as printer nozzle drilling [4] and flat panel display patterning [5]. Laser micromachining exploits the absorption of controlled amounts of photon energy by materials. The absorption mechanism is a complex, material and photon energy dependent, process. At low photon energies, such as those found in infra-red radiation, molecular vibration and rotation occurs leading to local heating of exposed areas of the material. Higher energies, such as those found at ultra-violet and smaller wavelengths, tend to lead to molecular dissociation and ionization processes. Accurate laser micromachining tends to use pulsed lasers at wavelengths where heating and melting-based surface disruption is minimal. By controlling the number of laser pulses, and hence the total incident radiation, precise machining depths can be achieved while minimal thermal distortion occurs at the edge of the exposed region.

In this work laser micromachining using nanosecond pulsed, ultra-violet (248nm) excimer and femtosecond pulsed infrared (800nm) lasers were used for the manufacturing stages in the creation of a microtitre array plate for electrokinetic assays capable of use with automated loading and measurement systems

2. Methods

2.1. Design

As with conventional microtitre plates, the electrokinetic platform comprised of a number of identical units arrayed on a single substrate. In this case 6 electrokinesis (combined dielectrophoresis and electrorotation) units were arrayed on a 75mm x 25mm substrate compatible with standard automated plate handling and sample loading systems. The starting point in designing the electrokinesis plate was the determination of a suitable microelectrode system that allowed both dielectrophoresis and electrorotation to be carried out in the same unit. A suitable electrode configuration is the quadrature polynomial electrode design of Huang *et al* [6]. Here four identical electrodes with a defined, curved, outline are arranged in a planar quadrature configuration. When adjacent electrodes are energised with sinusoidal voltages 180° out of phase with each other the electrodes form a non-uniform electric field in the central region of the inter-electrode space with a constant gradient in field strength. Energising the electrodes with sinusoidal signals 90° out of phase with each other creates a rotating electric field where the central region of the inter-electrode space has a near uniform electric field strength. To allow a suitably large number of cells to be examined at the same time in a single unit electrode system, while using easy to generate AC voltages of less than 20Vrms, the inter-electrode distance was chosen to be $400\mu\text{m}$. Such electrodes can be manufactured using a range of materials and methods. However, it has been found that fabrication using thin films produces an optimal electric field distribution both in the plane of the electrodes and extending away from the electrodes into the bulk sample liquid [7]. Figure 1a shows a diagram of the quadrature polynomial electrode configuration. Within the developed electrokinesis plate 6 identical microelectrodes and fluidic chamber units are linearly arranged equidistant along the major axis of the substrate. This simplifies automatic processing and also assists in the routing of electrical connection tracks between the active region of the microelectrodes and a single, 0.1 inch pitch, edge connector to give individual access to each electrode on the plate. Since the electrode components consisted of thin films, attention was given to the electrical resistance of each connection track. It is essential that each electrode in the quadrature arrangement is energised with an identical voltage to produce a rotationally symmetric electric field. Figure 1b shows the routing layout for the connection tracks of the electrokinetic microtitre plate. The edge connector contacts are 1.25mm wide on a 2.5mm pitch. The widths of tracks from the contacts to the active region of the microelectrodes have been reduced for electrodes closer to the edge connector to compensate for the shorter distance travelled and hence maintain a constant electrical resistance for all tracks.

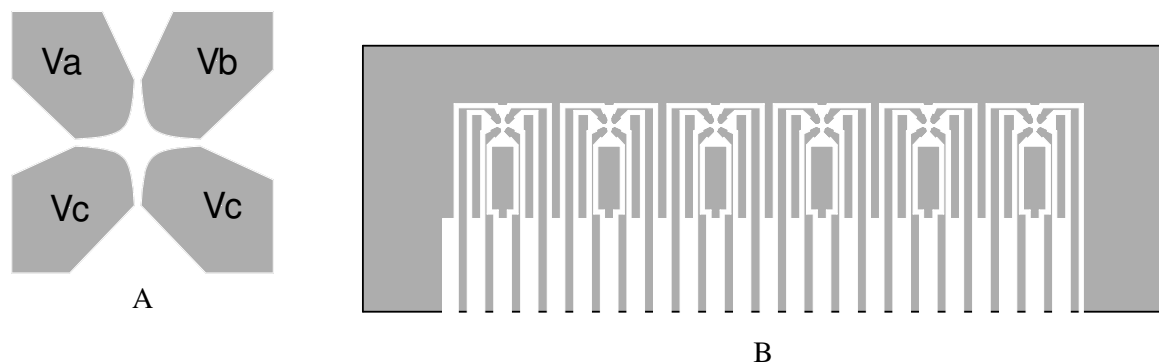


Figure 1 (A) A close up view of the quadrature polynomial microelectrode design with four energizing voltages Va, Vb, Vc and Vd indicated. (B) Electrokinetic microtitre plate layout showing 6 identical units on a single substrate. In both diagrams conducting regions are shown in grey.

The microelectrode array element of the electrokinesis plates takes the form of a planar substrate onto which electrodes typically $<1\mu\text{m}$ high have been produced. To allow the individual units to be

used independently, an open fluidic chamber system is required around each active electrode region. Such a chamber could be filled and possibly drained using either manual or automated dispensing systems. The active area of the electrodes is approximately 0.125mm^2 . Finite element analysis of the usable electric field produced by the thin film polynomial electrodes shows that it extends approximately $300\mu\text{m}$ above the electrodes when an aqueous sample occupies the electrokinesis unit. This gives an active volume of the unit of approximately 40nl . For accurate imaging-based analysis of electrorotation a maximum of approximately 100 cells should occupy this volume, so allowing the electrokinesis chamber to be used with sample concentrations up to 2.6×10^6 cells per ml. Accurate dispensing of such small volumes is still extremely difficult for both manual and automated systems. Therefore, the electrokinesis plate was required to hold significantly larger sample volumes for each unit but to physically constrain a 40nl volume over the electrode active region. This was achieved by the creation of a larger fluidic holding chamber above a smaller 40nl constraining chamber enclosing the active volume of the electrokinesis unit as shown in cross section in figure 2. The holding chamber is circular in nature with a 4mm diameter and 1mm depth allowing sample volumes of up to $50\mu\text{l}$ to be held. Such a volume is easily dispensed both by hand and automatically.

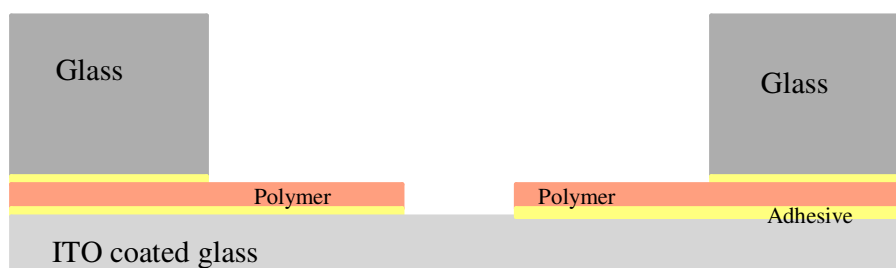


Figure 2 A cross sectional illustration of a single unit of the electrokinetic microtitre plate.

2.2. Materials

A recognised advantage of laser micromachining over many other microfabrication methods is its ability to structure an almost unlimited range of materials with the correct choice of laser. A range of substrate and electrode materials could be used for manufacturing the electrokinetic microtitre plates, all of which are suitable for laser micromachining. In this work it was intended that the movement of cells within each electrokinesis unit would be quantified by optical imaging techniques and may use fluorescence to highlight cells or distinguish between different cell populations. Therefore, an important consideration in choosing materials for the substrate and electrodes is maintaining a low background of UV-induced fluorescence. Glass was chosen as the substrate material for its transparent optical qualities, low fluorescence, mechanical strength and biocompatibility. Typically, glass substrate-based microelectrodes for electrokinesis have been manufactured from multilayer films such as gold on a chrome adhesion layer [8]. To assist in the imaging of the electrokinesis chamber it was desirable to have transparent electrodes. To this end, the electrodes employed in the electrokinesis platform were formed in a film of low resistance ($10\Omega/\text{sq}$) indium titanium oxide (ITO) film precoated onto a flat 1mm thick glass substrate (Delta Technologies Ltd. USA). ITO films have successfully been selectively laser micromachined on a glass substrate using excimer lasers for a number of applications such as display devices [5] and other electrokinetic cell analysis processes [9].

In fabricating and integrating the fluidic chamber over each unit, both chamber formation and bonding issues needed to be considered. The chamber must form a strong seal around the active region of the polynomial electrodes. To ensure an identical electrical path for the electric fields in each unit on the platform, fluid needed to be prevented from travelling between the ITO/glass substrate surface and the chamber forming layer surface by capillary action or any other means. To achieve this, a bilayer approach was adopted for forming the fluidic chambers. The upper holding chamber was formed from a single, 1mm thick glass sheet. As well as providing a biocompatible microfluidic

chamber, the glass plate also provides additional mechanical rigidity. The constraining chambers were formed in a single, adhesive backed, 250 μ m thick polymer sheet (Melinex A, Katco Ltd, UK)

2.3. Manufacture

Manufacture of the electrokinetic microtitre plates was carried out in two parts. The first used an excimer laser for the high resolution patterning of the ITO electrodes while the second used a femtosecond laser to trepan circular holes in the glass plate for the holding chambers and the adhesive backed polymer for the containment chambers. An important parameter in the manufacture of microelectrodes for electrokinetics is the edge quality of the field-producing electrodes. Since phenomena such as dielectrophoresis operate on non-uniformities in electric fields, roughness or patterning errors at the edge of electrodes are likely to produce unwanted electrokinesis. Excimer lasers produce large area beams with many thousands of modes which are likely to possess non-uniform intensity profiles. Machining of the ITO microelectrodes was carried out using an Exitech S8000 Excimer Laser Micromachining Workstation (Exitech Ltd. Oxford, UK). This system uses beam shaping and homogenising array optics to transform the output of a Lambda Physik Compex 110 excimer laser (Lambda Physik, Germany) into a 10mm x10mm uniform intensity beam at an image plane. The image plane is then projected through a demagnification lens onto the surface of a sample held at a workpiece plane. Using a projection lens with a magnification of x10, a workpiece beam of 1mm x 1mm in size and fluences of up to 10 Jcm⁻² can be created. To create the active region of the ITO electrodes, where the quality of the machined edge is of greatest importance, a mask projection machining process was used. Here, the curved polynomial electrode pattern was produced on a mask and positioned on a computer controlled XY positioning stage (Aerotech Inc., USA) with the mask surface at the image plane. As the mask is positioned at the image plane the electrode pattern was 10 times larger than the final features to be produced on the workpiece plane and, in covering the entire polynomial electrode region, measured approximately 40mm x 40mm. While it is typical to use patterned chrome on a quartz substrate masks for excimer laser micromachining, in this case a simple, low cost, polymer mask was employed. Excimer lasers produce light in the deep UV band, and most polymers will absorb such radiation. This is one of the reasons excimer lasers are so well suited to micromachining polymers. Therefore, low cost excimer laser masks can be produced using a polymer either as spin coated films on quartz or, as in this case, cutting a stencil in a polymer sheet. Since the mask dimensions were reasonably large, the mask was fabricated from a 200 μ m thick polymer sheet with the mask pattern cut out of the sheet using a femtosecond laser to give a mask resolution of approximately 10 μ m which, when projected onto the workpiece plane, produced a final electrode pattern resolution of 1 μ m – close to the optical imaging resolution of the S8000 workstation. To maintain rigidity, the stencil mask was held between two quartz plates. Employing a 248nm excimer laser, it was found that machining with a fluence of 1.5Jcm⁻² allowed the ITO film to be cleanly removed from the substrate with minimal damage to the underlying glass. To transfer the large mask pattern onto the workpiece plane a mask scanning-based machining technique was employed as illustrated in figure 3a. The ITO coated glass sample was held on a XYZ θ micropositioning stage (Aerotech Inc. USA) and both mask and workpiece motions were synchronised such that the position of the mask under the static laser beam corresponded to the appropriate position on the workpiece sample. Laser output firing was triggered on the movement of the workpiece stages by a defined incremental distance such that each laser output pulse overlapped with the previous pulse to produce a total laser exposure of 7.5jcm⁻².

Electrical connection tracks between the polynomial electrodes and the edge connector contacts were created by electrically isolating regions of the ITO coating using a direct write excimer laser micromachining process, as illustrated in figure 3b. The homogenised excimer laser beam was apertured at the image plane using a 4mm square aperture on a patterned chrome on quartz mask. Regions of ITO were isolated by moving the workpiece sample under the static, apertured, beam and triggering the laser output firing with incremental distance movement of the workpiece stages in both the X and Y direction. As with the mask scanning machining, a beam fluence of 1.5Jcm⁻² was used

with laser output being triggered to give a total exposure for machined areas of 7.5Jcm^{-2} . Workpiece motion was calculated from a computer aided design drawing of the electrical routing on the electrokinetic microtitre plate. The outlines of the electrical connections were translated into workpiece stage movements so allowing electrical isolation to be achieved by machining the outlines of the electrical connection tracks using the $400\mu\text{m}$ at the workpiece apertured beam.

To remove the possibility of short circuiting adjacent electrodes by misalignment of the external edge connector, ITO was completely removed from regions between the edge connector contacts. This was achieved by raster scanning the $400\mu\text{m}$ excimer laser beam over the area between each connector contact. To ensure all ITO was removed, adjacent machining actions overlapped by $200\mu\text{m}$, 50% of the beam width.

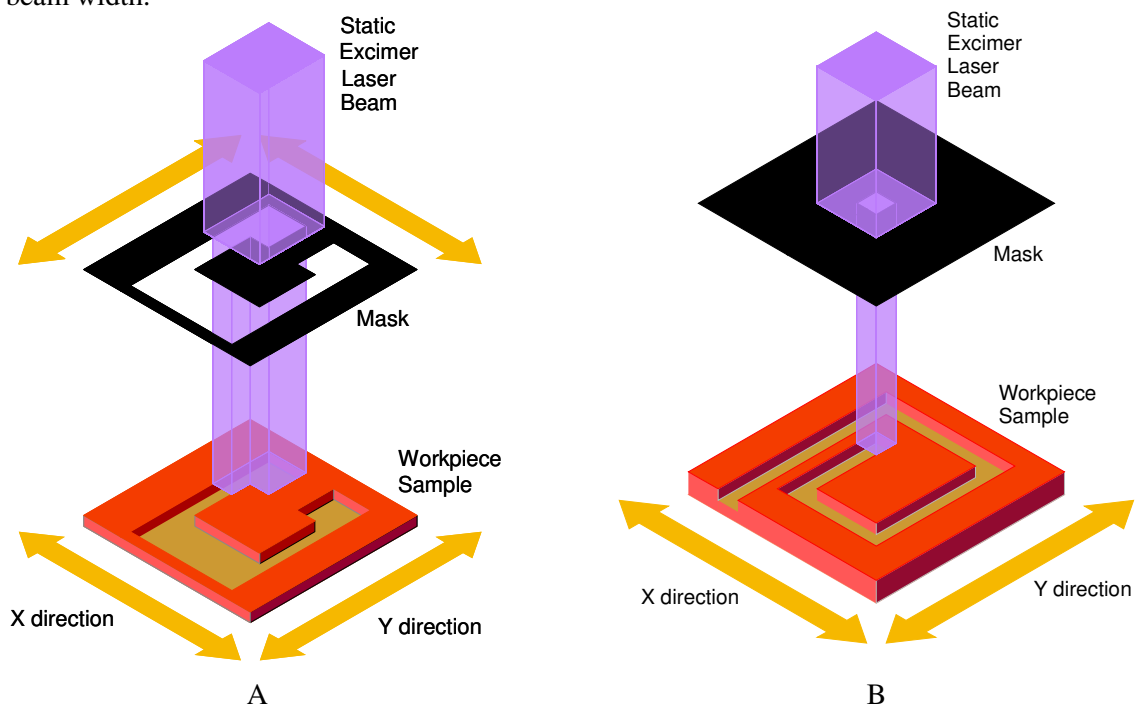


Figure 3. (A) An illustration of the principles of mask scanning laser micromachining. Mask motion is continuously synchronised with workpiece motion. (B) An illustration of direct writing excimer laser micromachining. The uniform large area beam is apertured by a static mask while the workpiece is moved. In both cases the laser beam is stationary and laser firing is triggered by incremental movement of the workpiece in either the X or Y direction.

The microfluidic chambers above the electrokinesis units were fabricated independently to the electrodes. 4mm diameter holes were laser machined using a Spectra Physics Hurricane Ti:Sapphire femtosecond laser integrated into an Exitech M2000F Laser Micromachining Workstation. This system delivered a tightly focussed pulses infra-red (800nm) light with a pulse duration of 120fs . The beam power density of up to 3.5Wcm^{-2} was focussed to a $20\mu\text{m}$ spot delivering power densities of up to 0.3MWcm^{-2} in a 120fs time period. Such high power densities have the ability to machine virtually any known material in a precise manner. The pulse duration is much shorter than the time required for heat to conduct away from the exposed area causing all the absorbed beam energy to be translated to an ionisation-based ablation process. The holes through the glass sheet that form the holding chambers were machined using a trepanning-based technique to machine a trench around the circumference of the hole. The complete hole is formed when the trench depth extends all the way through the glass sheet and the unmachined central portion of the hole is able to fall away. Hole machining was achieved using a beam power density of 30kWcm^{-2} and an effective workpiece velocity of 0.22mm/min .

The benefits of femtosecond laser micromachining are an extremely high cut edge quality with no significant machining debris. The lack of debris is of benefit when micromachining composite materials such as the adhesive backed polymer sheet used to form the containment chambers. The sheet comprised of a 250 μm thick polymer sheet coated on both sides with a 50 μm thick layer of adhesive which, in turn, was coated with a protective cover. Containment chamber holes were machined using a trepanning motion through the three materials, protective cover, adhesive and polymer sheet, in a single machining operation using a beam power density of 30kWcm⁻² and an effective workpiece velocity of 5mm/min. The ionising nature of the femtosecond laser ablation meant that all materials had similar ablation characteristics. In addition the small amount of debris produced in the machining operation was non-adhesive and could be fully removed from the sample prior to removal of the protective cover and assembly of the electrokinetic microtitre plates.

Final assembly of the device was carried out by first removing one layer of protective cover from the containment chamber sheet and then bonding the sheet to the holding chamber glass. The structure was then passed through a series of heated rollers at a temperature of 80°C to ensure full contact between the two surfaces. Next, the second protective cover was removed from the containment chamber sheet prior to alignment, using a modified mask aligner, and bonding to the ITO electrode substrate. Finally, the complete device was passed through the heated rollers to ensure a firm bond between all layers of the device.

3. Results and Discussion

Figure 4a shows the completed electrokinetic microtitre plate. The edge connector contacts can clearly be seen along the bottom edge of the device while the upper half of the device shows the six holding chambers and, in the centre of each chamber, the containment chambers. Figure 4b shows a close-up view of the ITO electrodes and the defocused outline of an enclosing containment chamber.

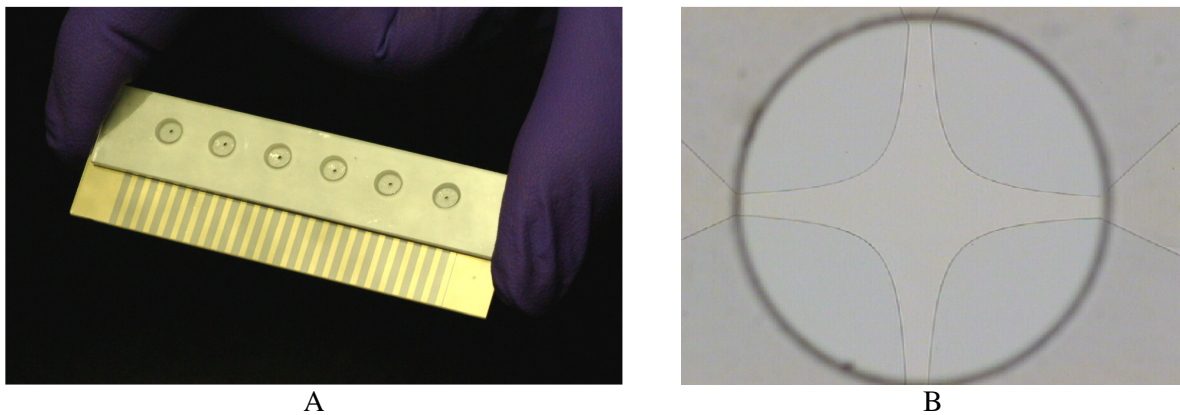


Figure 4 (A) Photograph of a completed electrokinetic microtitre plate with fluidic chambers. (B) Close-up view of the laser micromachined ITO polynomial electrodes. The defocused outline of the containment chamber is also visible surrounding the active region of the polynomial electrodes.

Microscopic observation of the edge of the laser machined ITO polynomial electrodes showed that an edge roughness of <100nm was achieved using the mask scanning micromachining process. Direct writing micromachining used to isolate the ITO electrical tracks between the polynomial electrodes and the edge connector produced an edge roughness of approximately 2 μm . This was largely due to small errors in the alignment of the edges of the 400 μm square beam with the X and Y axis of the workpiece stages causing an undulating edge as successive, adjacent, laser pulses are partially overlaid.

Measurements of the electrical resistance of the connection tracks between the active polynomial electrodes and the edge connector contacts gave a track resistance of 300 $\Omega \pm 10\Omega$. Such close resistances help ensure predictable and rotationally symmetrical electric field distribution within the

inter-electrode region. This is confirmed by experimental data from the negative dielectrophoretic collection of polystyrene latex beads within the electrode chambers as shown in figure 5a. It can be seen that beads are corralled into the centre of the interelectrode region to form a closely packed square body of particles. The uniform geometry of this collection with corners of the square aligned to the tips of adjacent electrodes, is evidence that the electric field produced by the each electrode is equal. Figure 5b shows experimental evidence that both positive and negative dielectrophoresis is possible within the units of the electrokinesis plate. Here live yeasts cells are collected using a positive dielectrophoretic force, while simultaneously latex beads are corralled at the centre of the electrodes. This selective separation is a result of the effective polarizability of the beads being less than that of the suspending medium which, in turn, is less than that of the yeast cells. The generally uniform distribution of cells on the electrode edges and the similar lengths to chains of collected cells is additional evidence of the good rotational symmetry of the produced electric field.

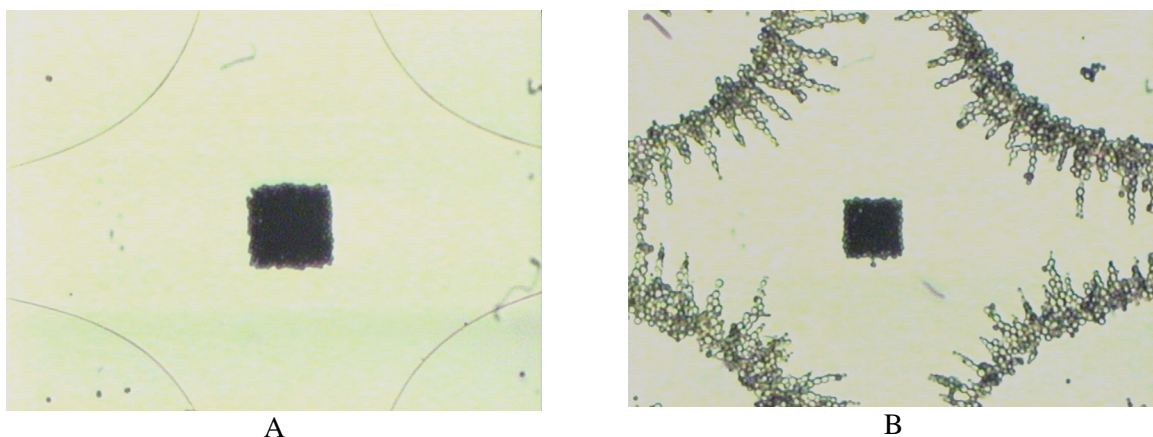


Figure 5 Developed electrokinetic microtitre wells in use. (A) The corraling of latex microbeads by negative dielectrophoresis. (B) Differential dielectrophoresis showing latex microbeads corralled by negative dielectrophoresis with simultaneous collection of yeast cells by positive dielectrophoresis.

For a given electric field configuration, both electrorotational and dielectrophoretic forces are frequency-dependent functions of the dielectric properties of the cell and suspending medium. Many electrokinetic studies examine the electrokinetic response of cells over a frequency range. Figure 6 shows the electrorotational and dielectrophoretic spectrum of live yeast cells collected using the electrokinetic microtitre plate. In this case energizing voltages of 5V_{pp} were applied to each electrode. The spectra shown in figure 6 are in close agreement with those of previous workers [10] and, for electrorotation, show a strong anti-field (negative) peak in rotation rate below approximately 1MHz and the start of a co-field peak in the rotation rate at frequencies above 1MHz.

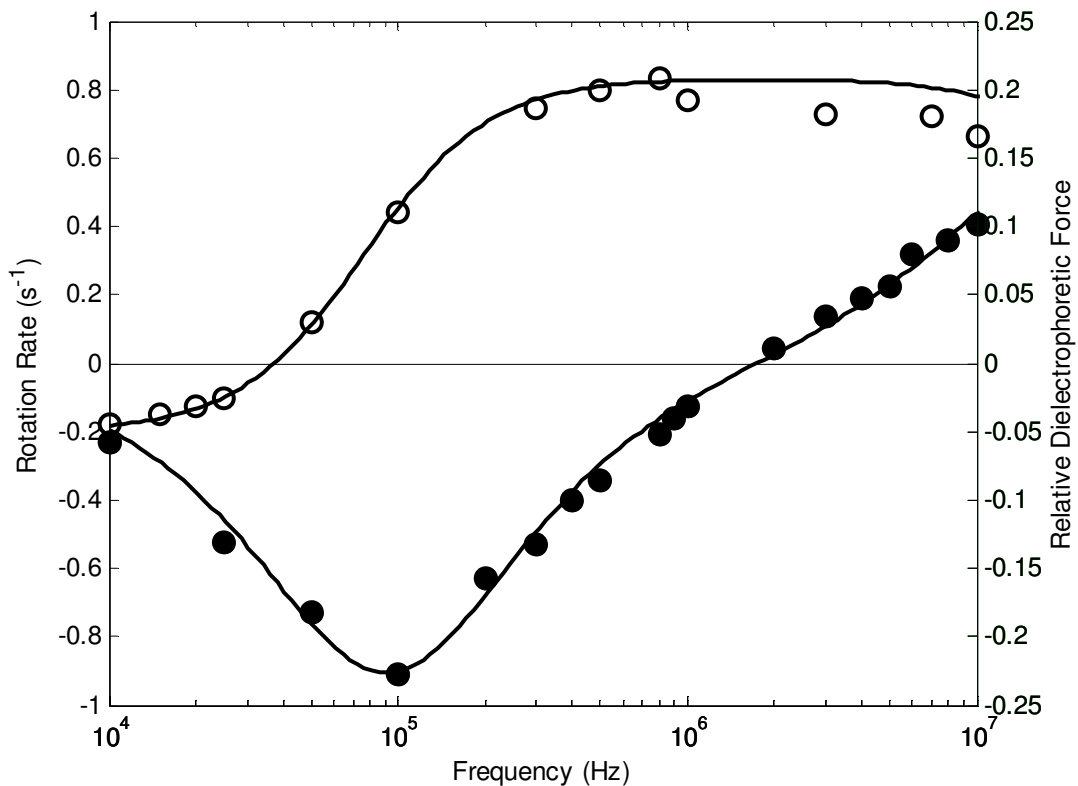


Figure 6 Electrorotation (●) and Dielectrophoretic (O) spectrum for live yeast cells. In both cases the suspending medium conductivity was $50\mu\text{S}/\text{cm}$. Voltages of 6V_{pp} were used for dielectrophoresis while 13V_{pp} was used for electrorotation studies

The devices fabricated in this work made use of an acrylic adhesive backed polymer sheet to bond the components of the electrokinetic microtitre plate together. Such adhesives can be sensitive to aqueous environments. Immersion tests of the fabricated devices revealed no observable deterioration in the strength of the devices or the seal around each containment chamber on immersion in water for one week. Similar devices have also been fabricated by us using polymer sheets pre-coated with a silicone adhesive if greater prolonged exposure to aqueous media is required.

4. Conclusions

The work described here has demonstrated the flexibility of laser micromachining for the complete fabrication of an electrokinetic microtitre plate, whose design and operation has been validated by conducting electrorotation and dielectrophoresis experiments on yeast cells. The processing has made use of the unique machining properties of two different types of lasers to produce an integrated device. While other manufacturing processes may be used to create parts of the devices, only laser micromachining has the ability to produce all components of the microtitre plates. The flexibility of laser micromachining coupled with the ability to use low cost stencil mask allows iterations in all aspects of device design to be quickly and cheaply realized. Variations in manufacturing material can easily be handled along with the quick production of stencil masks for evolutions in electrode design. Experimental validation data has shown that the described devices are equivalent to those manufactured using traditional photolithographic processes.

5. Acknowledgements

This work has been supported in part by the Optical Biochip Consortium (EPSRC award GR/S23483/01) and was commissioned by the University of Wales, Bangor using funds from the European Regional Development Fund and administered through the Welsh Assembly Government's Knowledge Exploitation Fund.

6. References

- [1] H. Morgan and N. Green (2001) AC Electrokinetics: Colloids and nanoparticles. Research Studies Press, Baldock.
- [2] R. Pethig (2006) 'Cell Physiometry Tools Based on Dielectrophoresis', in Ferrari, M. (Ed): 'BioMEMS and Biomedical Nanotechnology' (Springer, New York,), Vol.II, 103-126
- [3] M.Gower and N. Rizvi (2000) Applications of Laser Ablation to microengineering. *Proc. SPIE vol. 4065 High Power Laser Ablation III*.
- [4] M.C. Gower (2000) Excimer laser microfabrication and micromachining . *Prod. SPIE Vol. 4088* 124-131
- [5] P.T. Rumsby "Advanced laser tools for display device production on super large substrates", IMID 2002, Digest
- [6] Y. Huang and R. Pethig (1991) Electrode Design for Negative Dielectrophoresis. *Meas. Sci. Technol.* **2** 1142-1146
- [7] N. Green, A. Ramos and H. Morgan (2002) Numerical solution of the dielectrophoretic and travelling wave forces for interdigitated electrode arrays using the finite element method. *J. Electrostatics* **56**(2) 235-254
- [8] R. Pethig, J.P.H. Burt, A. Parton, N. Rizvi, M.S. Talary and J.A. Tame (1998) Development of Biofactory-on-a-Chip Technology using Excimer Laser Micromachining. *J. Micromech Microeng* **8** 57-63
- [9] J. Suehiro and R Pethig (1998) The dielectrophoretic movement and positioning of a biological cell using a three-dimensional grid electrode system. *J. Phys. D: Appl. Phys.* Vol. 31 22 3298-3305
- [10] R. Holzel (1997) Electrorotation of single yeast cells at frequencies between 100Hz and 1.6GHz. *Biophys. J.* **73**(2) 1103-1109